Eur. Phys. J. B **10**, 215–221 (1999)

THE EUROPEAN PHYSICAL JOURNAL B

EDP Sciences

Hypersonic wave anomalies in $Cs_3H(SeO_4)_2$ at the transitions above room temperature

Y. Luspin[a], D. De Sousa Meneses, P. Simon, and G. Hauret

Centre de Recherche sur les Matériaux à Haute Température, CNRS, 1D avenue de la Recherche Scientifique, 45071 Orléans Cedex 2, France

Received 16 October 1998

Abstract. The elastic properties of $Cs_3H(SeO_4)_2$ are investigated by Brillouin spectroscopy in the temperature range 20–220 °C covering the two transitions III → II and II → I occurring at ∼ 95 °C and ∼ 187 °C, respectively. Phase I is known to be a protonic conductive one. Discontinuities of elastic constants are generally observed at both transitions, implying first orderness. In phases II and I, a slight broadening of the Brillouin lines is detected. The results are discussed in comparison with compounds of the families $XHSeO_4$ (X = NH_4, Rb and Cs) and CsH_2BO_4 (B = As and P) which also undergo a transition to a superionic phase. In the conductive phase, it appears that the lattice anharmonicity is weaker in $Cs_3H(SeO_4)_2$ than in these other compounds.

PACS. 64.70.Kb Solid-solid transitions – 62.20.Dc Elasticity, elastic constants – 78.35.+c Brillouin and Rayleigh scattering; other light scattering

1 Introduction

Tricesium hydrogen biselenate $Cs_3H(SeO_4)_2$, usually abbreviated as TCHSe, belongs to a family of hydrogen-bonded compounds with the general formula $X_3H(AO_4)_2$ (X = NH_4, Rb, Cs and A = S, Se). These compounds undergo several phase transitions and attention has been recently paid to the transitions above room temperature [1–4], since one or two superionic phases have been found [5–9]. The conduction mechanisms have been discussed in connection with the structure and in comparison with other superionic compounds of the families $XHAO_4$, XH_2BO_4 (with B = P, As) and $X_5H_3(AO_4)_4$ [10–15].

The mechanism of the superionic transition in all these compounds is not elucidated until now. We have investigated the elastic behaviour of several members of the $XHAO_4$ and XH_2BO_4 families by Brillouin scattering, and found elastic constant discontinuities (up to 40%) in each of them [16–20], that imply first order transitions. Moreover, no pretransitional features are observed, except for CsH_2PO_4 [20]. Measurements of other physical properties, such as conductivity [8,21], dielectric and thermal properties [3], also led to first order transitions. Thus, we feel that further investigations are needed to check whether first orderness is a general characteristic of the superprotonic transition in these compounds where a group-subgroup relation holds for adjacent phases. Consequently, we intend to study the elastic behaviour in the compounds $X_3H(AO_4)_2$. Elastic constants are expected to be sensitive to the break of hydrogen bond network and to the subsequent rearrangement of the structure. The interest in these compounds is that the structure of their hydrogen bond network in the non-conductive phase is quite different from that in the other two families. It can be also emphasized that investigations of elastic properties by ultrasonic methods in $Rb_3H(SeO_4)_2$ and $(NH_4)_3H(SeO_4)_2$ leads to a quasi-continuous transition [22,23]. However, Brillouin scattering studies do not seem to corroborate that result [24–27].

Here, we report a Brillouin scattering study of the elastic properties in TCHSe, performed over a temperature range which includes the superionic transition. It is to be noted that the superionic transition investigation in this compound is complicated by the existence of an intermediate phase II between room temperature (phase III) and the superionic phase I. The crystallographic axes of phase II are rotated with respect to those of the room temperature phase III.

2 Experimental and crystal data

Brillouin scattering experiments were performed with a pressure scanned, triple pass plane Fabry-Perot interferometer (effective finesse 70, resolving power 760 000). The spectra are frequency calibrated with a Michelson interferometer in parallel. The light source is the $\lambda_o = 514.5$ nm line of a single frequency Ar-ion laser whose frequency is controlled by an iodine cell.

[a] e-mail: Yves.Luspin@univ-orleans.fr

TCHSe crystals were grown by very slow cooling of a saturated aqueous solution of Cs_2CO_3 and H_2SeO_4 in stoichiometric ratio. As-grown crystals are transparent pseudo-hexagonal plates and most of them display a polydomain structure under polarizing microscope. The samples were cut from single domain regions with parallelepipedal shape and several millimeters on all sides.

The structure of the room temperature phase (III) is monoclinic, space group C2/m [28,29]. The most recent values of the parameters are: $a_{\mathrm{mIII}} = 10.888\,3$ Å, $b_{\mathrm{mIII}} = 6.387\,7$ Å, $c_{\mathrm{mIII}} = 8.440\,4$ Å, $\beta_{\mathrm{mIII}} = 112.448°$ and $Z = 1$ for the primitive cell [30]. These data agree with previous values [28,29,31].

By heating above room temperature, TCHSe undergoes a first transition to phase II at $T_1 \cong 96\,℃$, and a second one to a phase I near $T_S \cong 183\,℃$ [6]. These transition temperatures are slightly higher than those given previously [3]. The structure of phase II is also monoclinic, space group A2/a, with $a_{\mathrm{mII}} = 11.037$ Å, $b_{\mathrm{mII}} = 6.415$ Å, $c_{\mathrm{mII}} = 16.062$ Å, $\beta_{\mathrm{mII}} = 102.69°$ at $\sim 127\,℃$ and $Z = 2$ for the primitive cell [32]. The structure of phase I is trigonal with space group $R\bar{3}m$, $a_{\mathrm{h}} = b_{\mathrm{h}} = 6.420(6)$ Å, $c_{\mathrm{h}} = 23.447(2)$ Å for the triple hexagonal cell at $\sim 197\,℃$ and $Z = 1$ for the unit cell [29]. Superionic conductivity has been found in this trigonal phase [6,7]; the conductivity in the plane $\perp c_{\mathrm{h}}$ is isotropic and considerably greater than that along c_{h} [8,21]. The respective directions of crystallographic axes in these three phases are known [33]. Another set of interrelations between them has been reported [34], but the data in phase II do not agree with the Brillouin line polarizations we observed in that phase, unlike the data in [33]. The binary axis b_{mII} lies along one of the three binary axes of phase I. In the same way, the binary axis b_{mIII} lies also along one of the three binary axes of phase I but is not colinear with b_{mII}. Then, starting from a given monodomain in phase III (room temperature), two possible directions (and consequently domains) could exist for b_{mII} above the transition III $\rightarrow$ II, but the angle between b_{mII} and b_{mIII} directions equals 60° in any case. It can be noted that (i) the structure of phase I is common to the highest temperature phase in all the family compounds, (ii) the phase III is specific to TCHSe since other members do not display a phase with the C2/m symmetry, the structure of their room temperature phase being A2/a (that of phase II in TCHSe), except for $X = NH_4$.

The structure analysis of these various phases [11,29, 33] has shown that the superionic phase I probably consists of SeO_4 tetrahedra joined by a system of disordered hydrogen bonds into a network of six-membered rings. Thus, each proton is dynamically disordered with a population of 1/3 among three equivalent positions. At the I $\rightarrow$ II transition, each proton orders and forms a hydrogen bond to only one of the three positions, giving rise to the existence of H-bonded SeO_4 dimers with two dimerization directions and leading to an order-disorder character for this transition. At the II $\rightarrow$ III transition, half of the protons break H-bonds and become involved in the same dimerization as the remaining ones; this transition corresponds to a switching of one of the two dimerization directions in phase II.

The refractive indices at λ_o, related to the investigated scattering geometries, were measured at room temperature. The cell parameters allow the determination of the mass density. At room temperature, we obtain $\rho = 4.197\ \mathrm{g\,cm^{-3}}$. In phases II and I, variations of -1.4% and -2.5% with respect to this value are obtained respectively. They probably imply discontinuities at the transitions. In computing the elastic constants from Brillouin shifts, taking into account that (i) no data are available on the temperature dependences of the refractive indices and (ii) these temperature dependences and that of the mass density may partially compensate, we used the room temperature values of the indices and the mass density at any temperature.

For the measurements the samples were immersed in silicone oil as index matching liquid. This decreases the stray light and provides a better temperature homogeneity. It also protects the surface from the atmosphere [35]. To avoid hysteresis effects and (or) possible deterioration of the optical quality of the samples when cooled through the transitions, all measurements were performed upon heating. In a preliminary investigation, we observed the onset of bubble formation in the oil above 220 ℃ which indicates water loss, therefore no measurements were made above this temperature. After cooling down to room temperature, the samples remain transparent but exhibit a polydomain structure under the polarizing microscope. Hence, a sample cannot be used in more than one heating run.

3 Brillouin experiments

The Brillouin spectra were collected in right-angle scattering geometry. The velocity V of an acoustic wave is then related to the corresponding frequency shift ν by:

$$V = \lambda_o \nu / \left(n_i^2 + n_s^2\right)^{1/2},$$

where n_i and n_s are the refractive indices for the incident and scattered light, respectively.

In phase III, the elastic constants are referred to orthogonal x, y and z axes chosen as follows: $x \| b_{\mathrm{mIII}}$, $y \| a_{\mathrm{mIII}}$ and $z \perp x$ and y. In phase I, these axes coincide with the usual frame of the trigonal phase, where x and z lie along a binary axis and the ternary axis, respectively. Then, the xyz frame is adequate for both phases I and III. Owing to the rotation of the binary axis by 60° at the III $\rightarrow$ II transition, this frame is less adequate in phase II, in which the set x^*, y^* and z^* with $x^* \| b_{\mathrm{mII}}$, $y^* \| a_{\mathrm{mII}}$ and $z^* \perp x^*$ and y^* would be more convenient. Nevertheless, it can be noted that z^* coincides with z and therefore the frame xyz is also useful in phase II for the direction $\perp a_{\mathrm{mII}}$ and b_{mII}.

Investigations *versus* temperature have been made on parallelepipedal samples which were cut and oriented so that the acoustic wave vector $\mathbf{q}$ lies along the x, y and z axes, in phases III and I, and x^* and z^* in phase II. The scattering geometries are listed in Table 1 with the expression for ρV^2 in terms of the elastic constants C_{ij}.

Table 1. The scattering geometries. The usual conventions for the wave vectors and polarization directions of the incident and scattered light are used. L (longitudinal), pL (pseudo-longitudinal), T (transverse), and pT (pseudo-transverse) relate to the nature of the acoustic waves. (1), (2), (3) and (4) are cumbersome expressions of ρV^2 in terms of elastic constants. (5): the same expression as in phase III in which the C_{ij} have to be replaced by the corresponding C^*_{ij}.

		Phase III			Phase II			Phase I		
Scattering geometries		**q** direction	Ac. wave nature	Expression for ρV^2	**q** direction	Ac. wave nature	Expression for ρV^2	**q** direction	Ac. wave nature	Expression for ρV^2
1	$(-x+y)[z,z](x+y)$ **q** // x	// b_{mIII}	L	C_{11}	in (001)* plane 60° from b_{mII}	pL	(2)	// a_h	L	C_{11}
2	$(-y+z)[x,x](y+z)$ **q** // y	// a_{mIII}	pL pT	$\{C_{22}+C_{44}+[(C_{22}-C_{44})^2+4C_{24}^2]^{1/2}\}/2$ $\{C_{22}+C_{44}-[(C_{22}-C_{44})^2+4C_{24}^2]^{1/2}\}/2$	in (001)* plane 30° from b_{mII}	pL pT	(3) (4)	$\perp a_h$ and c_h	pL pT	$\{C_{11}+C_{44}+[(C_{11}-C_{44})^2+4C_{14}^2]^{1/2}\}/2$ $\{C_{11}+C_{44}-[(C_{11}-C_{44})^2+4C_{14}^2]^{1/2}\}/2$
3	$(-y-z)[x,x](-y+z)$ **q** // z	$\perp$ (001) plane	pL	$\{C_{33}+C_{44}+[(C_{33}-C_{44})^2+4C_{34}^2]^{1/2}\}/2$	$\perp$ (001)* plane	pL	(5)	// c_h	L	C_{33}
4	$(-x\cos(75°)-y\cos(15°))$ $[z,z]$ $(-x\cos(15°)+y\cos(75°))$ **q** // $[-1/2, \sqrt{3}/2, 0]$	in (001) plane 60° from b_{mIII}	pL	(1)	// b_{mII}	L	C_{11}*	// a_h	L	C_{11} (=C_{11}*)

We concentrated on lines corresponding to longitudinal (L) or pseudo-longitudinal (pL) elastic waves because the lines related to transverse (T) or pseudo-transverse (pT) waves are generally weak or absent (except in geometry 2 in which the intensity of the line related to the pT wave is similar to that of the pL one). The measurement of refractive indices at room temperature gave $n_b = 1.593$ (active in geometries 2 and 3); for geometries 1 and 4, the values obtained for $[(n_i^2 + n_s^2)/2]^{1/2}$ are practically the same and equal to 1.575.

In scattering geometries 2 and 3, if we assume that C_{24} and C_{34} are small with respect to C_{22}-C_{44} and C_{33}-C_{44}, respectively, we have: $\rho V_y^2(\mathrm{pL}) \cong C_{22}$ and $\rho V_y^2(\mathrm{pT}) \cong C_{44}$ in phase III and I, and $\rho V_z^2(\mathrm{pL}) \cong C_{33}$ in phase III. In this last phase, this assumption is justified owing to the quasi-orthorhombic structure. With the choice of axes: $\mathbf{a}' = \mathbf{a}_{mIII}$, $\mathbf{b}' = \mathbf{b}_{mIII}$ and $\mathbf{c}' = \mathbf{a}_{mIII} + 3\mathbf{c}_{mIII}$, we obtain $\beta' = 87.03°$. Nevertheless, to test this assumption more quantitatively at room temperature, we performed additional measurements on the pT wave in geometry 3, and in another sample cut with its edges along x, y and z and **q** along [011] and [0$\bar{1}$1]. From the values of ρV_{pT}^2 and ρV_{pL}^2 obtained with **q** along [010], [001], [011] and [0$\bar{1}$1], those related to the last two directions being only used in the relation:

$$\rho\left\{V_{pL}^2[0\bar{1}1] + V_{pT}^2[0\bar{1}1] - V_{pL}^2[011] - V_{pT}^2[011]\right\} = 2\left(C_{24} + C_{34}\right),$$

the following results have been obtained (in GPa):

$$C_{22} = 35.9 \pm 0.7 \quad C_{33} = 30.9 \pm 0.6$$
$$C_{44} = 10.8 \pm 0.2 \quad C_{24} = 5.2 \pm 1 \quad C_{34} = 2.3 \pm 0.5$$

The estimated accuracy corresponds to 2%, except for C_{24} and for C_{34} where it equals 20%. Systematic relative shifts between ρV_y^2(pL) and C_{22}, ρV_z^2(pL) and C_{33}, and between ρV_y^2(pT) and C_{44}, are found equal to 2.9%, 0.8% and 9.5%, respectively. Then, it should be concluded that ρV_y^2(pL) and ρV_z^2(pL) have to be considered as weakly different from C_{22} and C_{33}, respectively, and that ρV_y^2(pT) differs significantly from C_{44}.

4 Results and discussion

4.1 Elastic constants

The temperature dependences of ρV^2 are reported in Figures 1 and 2. Owing to the monoclinic symmetry of phases II and III and the rotation of crystallographic axes at the III $\rightarrow$ II transition, depolarized lines are expected in several cases. The line polarizations, in agreement with expectation, are: (i) in phase III, depolarized lines in geometries 1 and 4, (ii) in phase II, depolarized lines in the four geometries, (iii) fully polarized lines in all other cases. The amount of depolarization depends on the case. As example, in phase II and geometry 3, the line intensities are practically the same in VH and VV polarizations, just below the II $\rightarrow$ I transition. This transition was directly observed by the abrupt decrease to zero of the intensity in the VH polarization.

Discontinuities are generally observed at the transitions, which are found at $T_1 = 95.5 \pm 0.5$ °C and $T_S = 187.5 \pm 0.5$ °C, in agreement with most previous values. For **q** along z, only a slight change of slope is observed at T_1, without discontinuity. In every phase, ρV^2 decreases

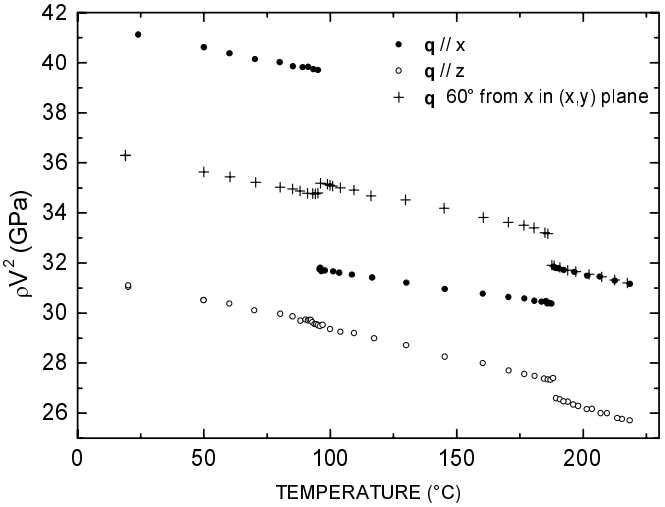

Fig. 1. Temperature dependences of ρV^2 for longitudinal or pseudo-longitudinal elastic waves active in scattering geometries 1 [$\mathbf{q}\|x$], 3 [$\mathbf{q}\|z$] and 4 [$\mathbf{q}\|$ in (001) plane at 60° from x].

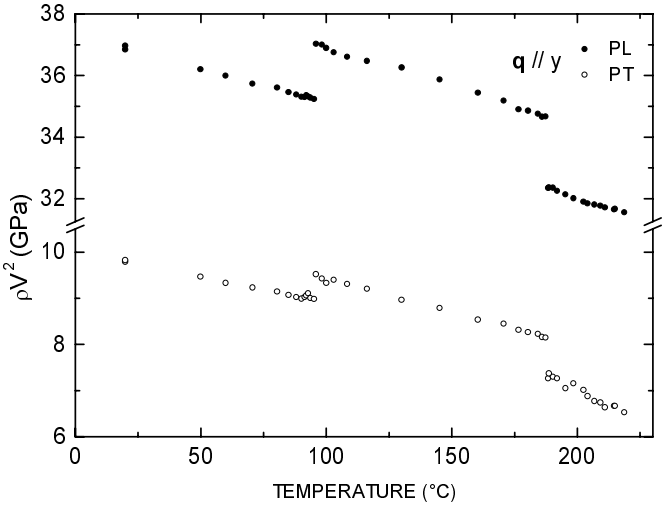

Fig. 2. Temperature dependences of ρV^2 for pseudo-transverse and pseudo-longitudinal elastic waves active in scattering geometry 2 [$\mathbf{q}\|y$].

linearly with T and no pretransitional features occur in the vicinity of the transitions.

In phase II, domains are expected to appear. However, whatever the domain, the angle between $\mathbf{q}$ and $\mathbf{b}_{\mathrm{mII}}$ is equal to 60° for $\mathbf{q}\|x$ and a single value for ρV^2 should be obtained, as experimentally observed (two different samples gave the same results). For $\mathbf{q}\|z$, the same remark can be made, but with a value for the angle equal to 30°. In the scattering geometry 4, $\mathbf{q}$ is expected to lie along $\mathbf{b}_{\mathrm{mII}}$ or to make an angle of 60° with it, depending on the type of domain. In the later case, the values of ρV^2 are also measured in geometry 1 and differ significantly from those obtained in geometry 4; therefore, it must be concluded that $\mathbf{q}$ lies along $\mathbf{b}_{\mathrm{mII}}$ in the investigated sample and that $\rho V^2 = C_{11}^*$, as reported in Table 1. The sample was translated to change the position of the scattering volume, but we could not observe the value of ρV^2 corresponding to the other type of domain.

In phase I, ρV^2 is expected to be equal to C_{11} in both geometries 1 and 4. This is in excellent agreement with the experimental results. In geometry 2, $\rho V_y^2(\mathrm{pL})$ and $\rho V_y^2(\mathrm{pT})$ allow the determination of C_{44} and $|C_{14}|$, which were found equal to 7.8 GPa and 3.6 GPa at 188 °C, respectively. Thus, it can be deduced that $\rho V_y^2(\mathrm{pL})$ and $\rho V_y^2(\mathrm{pT})$ are systematically shifted from C_{11} and C_{44} by +1.6% and −6.4%, respectively.

At T_1, the absence of discontinuity for ρV^2, for $\mathbf{q}$ along z, suggests that the structure modifications, which are known to take place mainly in (001) planes, essentially preserve the cohesion along z. Assuming that the difference between $\rho V_z^2(\mathrm{pL})$ and C_{33} in phase II is similar to that in phase III (0.8% at room temperature), a small downward shift of 2.2% would occur for C_{33} at T_{S}. This implies a weak change in the structure cohesion along z at the superionic transition. Only the elastic constant C_{11}^* can be directly measured in both phases I and II, showing the interest of geometry 4. A downward shift is observed as well for that constant at the superionic transition. In those cases where ρV^2 does not correspond to a unique elastic constant in phase II, it must be emphasized that a discontinuity of ρV^2 at T_{S} also reflects a first order transition, in spite of the discontinuous rotation of the crystallographic axes. Hence, the set of our results unambiguously corroborates the first order character of the superionic transition. The sign of the shift in any ρV^2 can be positive or negative, depending on its expression in terms of elastic constants. The interest of geometries in which ρV^2 corresponds to a unique elastic constant is that the sign of the shift in this elastic constant is directly obtained. Therefore, a straightforward comparison can be made with theoretical predictions.

In $Rb_3H(SeO_4)_2$ discontinuities in elastic constants are also observed in Brillouin scattering at the transition $A2/a \rightarrow R\bar{3}m$ [24,25]. When $\mathbf{q}$ lies along the binary axis of the monoclinic phase, an upward shift for the elastic constant (labelled C_{22} in these papers) is observed, unlike our result in TCHSe (the corresponding constant is C_{11}^*). In ultrasonic studies, a downward continuous decrease is observed [22]. Moreover, different values for C_{22} are obtained just above the transition: $\sim$ 35 GPa by ultrasonic method and $\sim$ 43 GPa by Brillouin scattering. This was attributed to dispersion [26]. A possible explanation of this effect was given in terms of a bilinear interaction between the protons and the elastic waves [36]. This interaction, assumed to be active at ultrasonic frequencies but not at hypersonic ones, can lead to the observed quasi-continuous variation for C_{22} near T_{S} observed in ultrasound. A similar dispersion also appears in $(NH_4)_3H(SeO_4)_2$ [23–27].

4.2 Brillouin linewidths

In phase III, no broadening of the Brillouin lines was detected. But in phases II and I, weak broadenings are observed for every line related to a L or pL acoustic wave. As

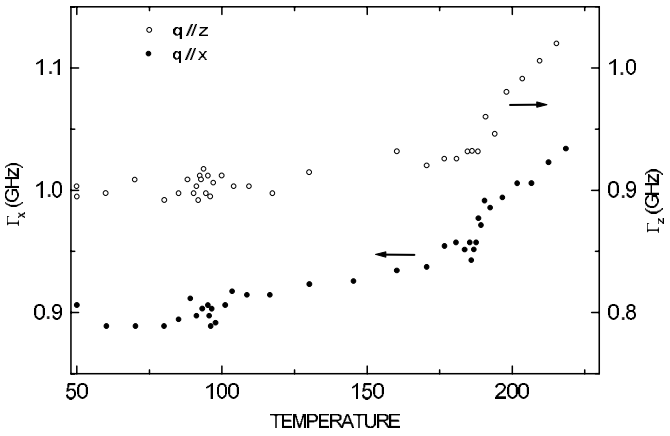

Fig. 3. Temperature dependences of Γ_x and Γ_z, FWHM of the Brillouin line related to the longitudinal and pseudo-longitudinal waves propagating along x and z, respectively.

example, the full width at half maximum (FWHM) Γ_x and Γ_z of the lines corresponding to $\mathbf{q}\|x$ and $\mathbf{q}\|z$ are reported in Figure 3, without deconvolution. In both phases, quasi-linear increases take place, without discontinuity at T_S or pretransitional features in the vicinity of the transitions.

In the superionic phase, the maximum value of the linewidths observed at the highest investigated temperature is estimated to 0.2 GHz, after deconvolution. This value is significantly lower than those observed in $CsHSeO_4$ [18], CsH_2AsO_4 [19] or CsH_2PO_4 [20] which lie in the frequency range 0.5–2 GHz, depending on the compound and the line. In these last compounds, we discussed the consequences of a bilinear coupling between acoustic waves and mobile protons [18–20]. It was concluded that, at Brillouin frequencies ($\sim$ 10 GHz), this coupling cannot explain the value of the broadenings and that an effect on the elastic constants would be too small to be observed. Therefore, the assumption of a strong anharmonicity was proposed as a possible explanation of the broadenings [18–20]. In TCHSe, the characteristics of the mobile protons are similar to those in the last compounds. The proton relaxation time τ_p can be estimated from conductivity measurements [8]. From the conductivity data in the plane orthogonal to the ternary axis, a value of about 0.3 GHz can be obtained for $(\tau_p)^{-1}$. As shown in [20], the contribution of mobile protons to Brillouin linewidths is $\Gamma = \alpha(\tau_p)^{-1}$, with $\alpha < 1$. From data in $Rb_3H(SeO_4)_2$ [26], the coefficient $\alpha \sim 0.1$ is estimated. In TCHSe, a similar value can be expected, making that contribution negligible. Moreover, this contribution would be temperature independent, in disagreement with the temperature dependence of the broadenings in the superionic phase. Thus, we think that the total broadening should also be attributed to lattice anharmonicity. Owing to the values for the broadenings, which are significantly lower in TCHSe than in the compounds belonging to the other two families $XHSeO_4$ and CsH_2BO_4, we conclude to a weaker anharmonicity in TCHSe than in these compounds. In phase II, in which no (or only a small) contribution of mobile protons is expected, we think that the broadenings can be also attributed to anharmonicity. An increase of anharmonic interactions in both phases I and II is also supported by the IR reflectivity results, showing that all modes are appreciably broader in phases I and II than in phase III [37].

It can be noted that the temperature behaviour of the linewidths we obtain in TCHSe near the II $\rightarrow$ I transition is different from that observed in $Rb_3H(SeO_4)_2$ [25], where in particular, a slight decrease of the width takes place upon heating above T_S.

4.3 Elastic Rayleigh peak

At room temperature, typical values of the ratio $R = I_R/I_B$, I_R and I_B being the intensities of the Rayleigh and Brillouin (related to a L or pL acoustic wave) peaks in a given spectrum, are of about 2–30, depending on the sample and on the scattering geometry. At T_1, a discontinuous increase of R occurs in every sample to values of about 2×10^3 to 9×10^3. A visual inspection of the beam path in the sample suggests a quasi-homogeneous deterioration of the optical quality. At T_S, no further change occurs for I_R. Then, the strong increase of I_R at T_1 cannot be attributed to the possible appearance of domain walls in phase II since (i) the walls shall disappear at T_S, (ii) translations of the samples in phase II do not reduce I_R. This increase might be likely due to a great number of static defects which are generated by the structural change.

In phase I, the mobile protons perform diffusion jumps [11,14]. They are expected to give a relaxational quasi-elastic peak in the scattering spectra. The width Γ_p of this peak, which is given by $\Gamma_p = (\tau_p)^{-1}/\pi$, is of about 0.1 GHz. This value is lower than the apparatus width Γ_a (0.9 GHz). Therefore, this quasi-elastic peak, if it arises with detectable intensity, would be added to the elastic Rayleigh peak. But, the important value of I_R in the conducting phase cannot be attributed to this quasi-elastic peak since (i) the increase of I_R occurs at T_1, (ii) the large value of I_R persists after the samples are cooled down to room temperature.

4.4 Discussion of the transitions

Unlike most compounds of the $XHAO_4$ and XH_2BO_4 families, in which the symmetry of the superionic phase has not been investigated or not confirmed, the symmetries of the various phases of TCHSe are well known. Since a group-subgroup relation holds, the transition $R\bar{3}m \rightarrow A2/a$ (I $\rightarrow$ II), which also occurs in $Pb_3(PO_4)_2$, has been group-theoretically analyzed [38] and applied to TCHSe [39,40]. An analysis of the possible ordering of protons below the superionic transition showed that the phase transition can be induced by two irreducible representations of $R\bar{3}m$ with different wave vectors: $\tau_3(\mathbf{K} \neq 0)$ and $E_g(\mathbf{K} = 0)$ [41], to which correspond two order parameters. As in this case several successive phases transitions are expected [42], this analysis has been applied to TCHSe [43]. Unfortunately,

wrong space groups were considered and the observed phase succession cannot be predicted.

In the framework of a transition induced by two order parameters, a qualitative discussion of the experimental results at the superionic transition can be given. The couplings between the symmetric strains e_i ($i = 1$ to 3) with the order parameter components Q_{1j}, corresponding to the irreducible representation τ_3, are $e_i Q_{1j}^2$ [38, 39]. Bilinear couplings $e_i Q_{2k}$ are allowed in the case of the second order parameter components Q_{2k} corresponding to the irreducible representation E_g. However, their effects on elastic constants would be very small at Brillouin frequencies, as in $Rb_3H(SeO_4)_2$ [26], and the next couplings $e_i Q_{2k}^2$ must be considered. Therefore, one has the well known coupling eQ^2 encountered in many cases (see [44] for a general review). Upon heating, this coupling gives rise to an upward step at the transition, which can be more or less relaxed in a dynamical regime. Obviously, this jump is of inverse sign to that experimentally observed for C_{11}^* and thus this coupling term cannot explain it. Therefore we must seek higher order couplings. The next one, generally allowed by symmetry, is he^2Q^2. This term gives several contributions to elastic anomalies among which, below the transition, a static one proportional to the equilibrium value of the order parameter squared Q_o^2 [44]:

$$\Delta C = C - C_o = 2hQ_o^2,$$

where C_o is the bare elastic constant. In the case of a positive coefficient h, a downward jump is expected for the elastic constant on heating through the (first order) transition. This jump, which would reflect that of Q_o^2, is in qualitative agreement with the experimental results. It is interesting to recall that, in the curves showing the temperature dependences of elastic constants below the superionic transition, a bending was only observed in CsH_2PO_4 [20]. This bending qualitatively agrees with the increase and saturation of the order parameter squared, which generally occurs on cooling below a transition. It was an argument in favour of a contribution of the he^2Q^2 coupling, which we are led to also invoke in the case of TCHSe.

Concerning the III $\rightarrow$ II transition, both C2/m and A2/a are subgroups of $R\bar{3}m$, but they are not themselves related by a group-subgroup relation. Thus, this transition corresponds to a first order one between two low-symmetry phases derived from a same parent phase. Such transitions, considered as reconstructive ones, generally involve large displacements of atoms [42]. These predictions agree with the absence of pretransitional features for every ρV^2 and with the generally observed discontinuities at this transition.

5 Conclusion

The present investigation shows that the elastic properties of TCHSe are sensitive to both transitions above room temperature. At the superionic transition, elastic constant discontinuities occur without pretransitional features, implying a first order one, as was also concluded in most of the $XHAO_4$ and XH_2BO_4 families compounds, and in Rb_3HSeO_4.

Within the assumption of transitions associated with order parameters, we propose a possible qualitative explanation for the elastic constant jumps at T_S, based on the static contribution of the he^2Q^2 coupling.

Small Brillouin line broadenings in both phases I and II show that anharmonicity in the lattice dynamics increases in phase II, in agreement with IR results. In the superionic phase, it turns out that these broadenings are significantly smaller than in the compounds $XHSeO_4$ (with X = NH_4, Rb and Cs) and CsH_2BO_4 (with B = As and P). This suggests a weaker disorder in TCHSe than in these other compounds.

To improve the knowledge of the superionic transition in TCHSe, we think that a widened study of other lattice modes will be required, such as IR reflectivity with a complete analysis, Raman scattering, and even neutron scattering (especially at the soft point in the Brillouin zone in the conducting phase), despite the incoherent scattering due to protons.

References

1. M. Ichikawa, J. Phys. Soc. Jap. **45**, 355 (1978).
2. M. Ichikawa, J. Phys. Soc. Jap. **47**, 681 (1979).
3. M. Komukae, T. Osaka, T. Kaneko, J. Phys. Soc. Jap. **54**, 3401 (1985).
4. T. Osaka, Y. Makita, K. Gesi, J. Phys. Soc. Jap. **46**, 577 (1979).
5. A.I. Baranov, I.P. Makarova, L.A. Muradyan, A.V. Tregubchenko, L.A. Shuvalov, V.I. Simonov, Sov. Phys. Crystallogr. **32**, 400 (1987).
6. A.I. Baranov, A.V. Tregubchenko, L.A. Shuvalov, N.M. Shchagina, Sov. Phys. Sol. State **29**, 1448 (1987).
7. A.I. Baranov, B.V. Merinov, A.V. Tregubchenko, L.A. Shuvalov, N.M. Shchagina, Ferroelectrics **81**, 187 (1988).
8. A. Pawlowski, Cz. Pawlaczyk, B. Hilczer, Solid State Ionics **44**, 17 (1990).
9. K. Furukawa, S. Akahoshi, T. Fukami, K. Hukuda, J. Phys. Soc. Jap. **59**, 4560 (1990).
10. Y.N. Moskvich, A.M. Polyakov, A.A. Sukhovsky, Ferroelectrics **81**, 200 (1988).
11. B.V. Merinov, A.I. Baranov, L.A. Shuvalov, Sov. Phys. Crystallogr. **35**, 200 (1990).
12. A.I. Baranov, Bull. Acad. Sci. USSR Phys. Ser. **51**, 60 (1987).
13. A.I. Baranov, B.V. Merinov, A.V. Tregubchenko, V.P. Khiznichenko, L.A. Shuvalov, N.M. Shchagina, Solid State Ionics **36**, 279 (1989).
14. R. Sonntag, R. Melzer, K.S. Knight, Physica B **234-6**, 89 (1997).
15. F. Kadlec, Y. Yuzyuk, P. Simon, M. Pavel, K. Lapsa, P. Vanek, J. Petzelt, Ferroelectrics **176**, 179 (1996).
16. Y. Luspin, Y. Vaills, G. Hauret, Solid State Commun. **84**, 847.(1992).
17. Y. Luspin, Y. Vaills, G. Hauret, Ferroelectric Lett. **18**, 99 (1994).

18. Y. Luspin, Y. Vaills, G. Hauret, Solid State Ionics **80**, 277 (1995).
19. Y. Luspin, Y. Vaills, G. Hauret, J. Phys. I France **6**, 941 (1996).
20. Y. Luspin, Y. Vaills, G. Hauret, J. Phys. I France **7**, 785 (1997).
21. B. Hilczer, A. Pawlowski, Ferroelectrics **104**, 383 (1990).
22. B.V. Shchepetil'nikov, A.I. Baranov, L.A. Shuvalov, N.M. Shchagina, Sov. Phys. Sol. State **32**, 1676 (1990).
23. B.V. Shchepetil'nikov, L.A. Shuvalov, A.V. Tregubchenko, Sov. Phys. Sol. State **34**, 236 (1992).
24. S.G. Lushnikov, S.D. Prokhorova, L.A. Shuvalov, Bull. Acad. Sci. USSR Phys. Ser. **53**, 78 (1989).
25. S.G. Lushnikov, I.G. Siny, Ferroelectrics **106**, 237 (1990).
26. S.G. Lushnikov, L.A. Shuvalov, Ferroelectrics **124**, 409 (1991).
27. M. Drozdowski, K. Lapsa, P. Ziobrowski, M. Augustyniak, Proc. of the SPIE-Int. Soc. Opt. Eng. **3178**, 255 (1997).
28. B.V. Merinov, A.I. Baranov, A.V. Tregubchenko, L.A. Shuvalov, Sov. Phys. Dokl. **33**, 715 (1988).
29. B.V. Merinov, N.B. Bolotina, A.I. Baranov, L.A. Shuvalov, Sov. Phys. Crystallogr. **33**, 824 (1988).
30. R. Sonntag, R. Melzer, T. Wessels, P.G. Radaelli, Acta Cryst. C **53**, 1529 (1997).
31. M. Ichikawa, T. Gustafsson, I. Olovsson, Acta Cryst. B **48**, 633 (1992).
32. B.V. Merinov, N.B. Bolotina, A.I. Baranov, L.A. Shuvalov, Sov. Phys. Crystallogr. **36**, 639 (1991).
33. M. Ichikawa, T. Gustafsson, I. Olovsson, J. Mol. Struct. **321**, 21 (1994).
34. M. Komukae, K. Sakata, T. Osaka, Y. Makita, J. Phys. Soc. Jap. **63**, 1009 (1994).
35. J. Grunberg, S. Levin, I. Pelah, D. Gerlich, Phys. Stat. Sol. (b) **49**, 857 (1972).
36. V.S. Vikhnin, S.G. Lushnikov, Ferroelectrics **167**, 109 (1995).
37. V. Zelezny, J. Petzelt, Y.G. Goncharov, G.V. Kozlov, A.A. Volkov, A. Pawlowski, Solid State Ionics **36**, 175 (1989).
38. J. Torres, Phys. Stat. Sol. (b) **71**, 141 (1975).
39. N.M. Plakida, W. Salejda, Phys. Stat. Sol. (b) **148**, 472 (1988).
40. D. Abramic, J. Dolinsek, R. Blinc, L.A. Shuvalov, Phys. Rev. B **42**, 442 (1990).
41. W. Salejda, N.A. Dzhavadov, Phys. Stat. Sol. (b) **158**, 119 (1990).
42. J.C. Toledano, P. Toledano, *The Landau theory of phase transitions* (World Scientific, Singapour, New Jersey, Hong Kong, 1987).
43. W. Salejda, N.A. Dzhavadov, Phys. Stat. Sol. (b) **158**, 475 (1990).
44. W. Rehwald, Adv. Phys. **22**, 721 (1973).